Published in final edited form as:
Mol Microbiol. 2012 September ; 85(6): 1148–1165. doi:10.1111/j.1365-2958.2012.08165.x.

Mycobacterium tuberculosis WhiB4 regulates oxidative stress response to modulate survival and dissemination *in vivo*

Manbeena Chawla[1,¶], **Pankti Parikh**[1,¶], **Alka Saxena**[1], **Mohamed Husen Munshi**[1], **Mansi Mehta**[1], **Deborah Mai**[2], **Anup K. Srivastava**[2], **K. V. Narasimhulu**[3], **Kevin E. Redding**[4], **Nimi Vashi**[1], **Dhiraj Kumar**[1], **Adrie JC Steyn**[2,#], and **Amit Singh**[1,*]

[1]Immunology Group, International Centre for Genetic Engineering and Biotechnology, New Delhi, India, 110067

[2]Department of Microbiology, University of Alabama at Birmingham, Birmingham, USA, 35294

[3]Pediatric Hematology & Oncology Research, St. Joseph's Children's Hospital Tampa, FL 33607

[4]Department of Chemistry and Biochemistry, Arizona State University, USA, 85287

[#]KwaZulu-Natal Research Institute for Tuberculosis and HIV (K-RITH), Durban, 4001, South Africa

Abstract

Host-generated oxidative stress is considered one of the main mechanisms constraining *Mycobacterium tuberculosis* (*Mtb*) growth. The redox-sensing mechanisms in *Mtb* are not completely understood. Here we show that WhiB4 responds to oxygen (O_2) and nitric oxide (NO) via its 4Fe-4S cluster and controls the oxidative stress response in *Mtb*. The WhiB4 mutant (*MtbΔwhiB4*) displayed an altered redox balance and a reduced membrane potential. Microarray analysis demonstrated that *MtbΔwhiB4* over-expresses the antioxidant systems including alkyl hydroperoxidase (*ahpC-ahpD)* and rubredoxins (*rubA-rubB*). DNA binding assays showed that WhiB4 [4Fe-4S] cluster is dispensable for DNA binding. However, oxidation of the apo-WhiB4 Cys thiols induced disulfide-linked oligomerization, DNA binding and transcriptional repression, whereas reduction reversed the effect. Furthermore, WhiB4 binds DNA with a preference for GC-rich sequences. Expression analysis showed that oxidative stress repressed *whiB4* and induced antioxidants in *Mtb*, while their hyper-induction was observed in *MtbΔwhiB4. MtbΔwhiB4* showed increased resistance to oxidative stress *in vitro* and enhanced survival inside the macrophages. Lastly, *MtbΔwhiB4* displayed hypervirulence in the lungs of guinea pigs, but showed a defect in dissemination to their spleen. These findings suggest that WhiB4 systematically calibrates the activation of oxidative stress response in *Mtb* to maintain redox balance, and to modulate virulence.

Introduction

The success of *Mtb* as a human pathogen hinges on its ability to latently infect ~2 billion people worldwide and then potentially reactivating in a subset of infected individuals. Molecular mechanisms underlying *Mtb* persistence and reactivation remain poorly understood, but are critical towards the development of novel strategies against tuberculosis (TB) infection. The production of reactive oxygen and nitrogen intermediates (ROI and

[*]Correspondence: Amit Singh, Wellcome/DBT India Alliance Intermediate Fellow, International Centre for Genetic Engineering and Biotechnology, Aruna Asaf Ali Marg, New Delhi-110067, Tel: 91-11-26741358, Fax: 91-11-26742316 asingh@icgeb.res.in.
[¶]These authors contributed equally to this work.

Conflict of Interests: We declare that no conflict of interests exists.

RNI, respectively) by macrophages is considered to be the major mechanism restraining *Mtb* proliferation *in vivo* (MacMicking *et al.*, 1997, Ng *et al.*, 2004). ROI and RNI generate intracellular redox stress and kill bacteria by damaging biomolecules such as DNA, proteins, and lipids. Studies have shown that nitric oxide synthase-2 (NOS2) and phagocyte oxidase (PHOX) gene knock-out mice are defective in generating RNI and ROI, respectively, and exhibit increased sensitivity to *Mtb* infection (MacMicking *et al.*, 1997, Cooper *et al.*, 2000). The importance of ROI in controlling *Mtb* infection in humans came from the observation that children with defective oxidative burst mechanisms are highly susceptible to TB and develop severe complications from BCG vaccination (Lee *et al.*, 2008). Despite these redox-based bactericidal stresses, *Mtb* can persist for decades in a non-replicative state *in vivo*. These studies suggest that *Mtb* genes involved in resistance to oxidative or nitrosative stress would play a role in persistence. However, the underlying mechanism of how oxidative and nitrosative stress is sensed by *Mtb* to coordinate the expression of virulence genes for persistence is poorly understood.

Thiol and/or Fe-S cluster based transcription factors such as OxyR and SoxR are known to sense oxidative and/or nitrosative stress in bacteria. OxyR responds to peroxide stress by a thiol-disulfide redox switch and controls the transcription of antioxidant systems such as catalase (KatG) and alkyl hydroperoxide reductase (AhpCF) (Green and Paget, 2004). SoxR regulates the expression of a large number of stress-responsive genes by sensing nitrosative and oxidative stress via its redox-responsive 2Fe-2S cluster (Green and Paget, 2004). OxyR and SoxR homologs are found in many bacterial species. However a prototypical homolog of SoxR is absent in the *Mtb* genome, and OxyR is nonfunctional due to the presence of multiple mutations in its open reading frame (ORF) (Deretic *et al.*, 1995). The absence of these regulators in *Mtb* is very intriguing and indicates that *Mtb* might possess novel redox-sensing proteins to control its survival in response to ROI/RNI stress during infection.

Recent studies suggest that *Mtb* is capable of sensing redox signals, such as O_2 and NO, via the heme-based DosR/S/T system, thiol-based SigH/RshA system, in addition to the family of Fe-S cluster-containing WhiB proteins (den Hengst and Buttner, 2008). The WhiB proteins are putative transcription factors that have been shown to regulate diverse functions, including pathogenesis, cell division, oxidative stress, nitrosative stress, reductive stress, disulfide reductase, and antibiotic resistance (Farhana *et al.*, 2010). These studies suggest that WhiB proteins might have a functional role in *Mtb* that is similar to OxyR and SoxR in other bacteria. Several studies have indicated an important function of WhiB4 in the pathophysiology of *Mtb*. For example, WhiB4 is induced during long-term hypoxia (Rustad *et al.*, 2008) and upon nutrient starvation (Betts *et al.*, 2002). WhiB4 expression is also influenced by oxidants (diamide and cumene hydroperoxide [CHP]), SDS, ethanol, isoniazid (INH), and inside macrophages (Geiman *et al.*, 2006, Rachman *et al.*, 2006). However, the molecular function of WhiB4 in *Mtb* remains uncharacterized.

In this study, we comprehensively analyzed the redox state and the O_2- and NO-sensing properties of the WhiB4 Fe-S cluster using low temperature EPR. We performed global microarray analysis to identify genes controlled by WhiB4. We systematically analyzed the capacity of WhiB4 to bind to the promoter regions of antioxidant genes in a redox-dependent manner, examined the sequence preference for WhiB4 DNA binding, and investigated the effect of DNA binding on transcription. Lastly, we examined the ability of *MtbΔwhiB4* to survive oxidative stress *in vitro*, inside macrophages, and during infection of guinea pigs. Collectively, our findings provide a fresh mechanistic insight into how *Mtb* responds to host generated redox stress via WhiB4 for survival *in vivo*.

Results

WhiB4 contains a redox-responsive [4Fe-4S] cluster as a cofactor

A hexahistidine-tagged version of WhiB4 was expressed in *E. coli* and purified from the soluble fraction by immobilized-metal affinity chromatography. Purified WhiB4 was light brown in color and displayed broad visible absorption maxima at approximately 330, 420, and 450 nm (Fig. 1A), which are characteristics of proteins containing bacterial type 2Fe-2S ferredoxins (Ta and Vickery, 1992). Since Fe-S clusters are sensitive to degradation during aerobic purification, we reconstituted the Fe-S cluster of WhiB4 under anaerobic conditions using the NifS-catalyzed procedure as reported previously (Singh *et al.*, 2007). During anaerobic reconstitution of WhiB4 Fe-S cluster, we observed a yellowish brown product along with a time-dependent increase in the absorption intensity at ~420 nm with no other resolved features (Fig. 1B). These spectral features are consistent with the presence of a FNR-type 4Fe-4S cluster in WhiB4 (Khoroshilova *et al.*, 1997).

Next, we examined the redox state of the 4Fe-4S cluster in WhiB4 by echo-detected field sweep EPR (EDFS-EPR). The anaerobically reconstituted WhiB4 was EPR silent, suggestive of the presence of an antiferromagnetically-coupled $[4Fe\text{-}4S]^{2+}$ cluster. Treatment with excess sodium dithionite (DTH) at pH 7.5 caused partial bleaching of the protein's yellowish brown color (data not shown) and resulted in a fast-relaxing axial EPR spectrum with *g*-tensor components of 2.06 and 1.94 (Fig. 1C). This signal was only observed below 10 K and is consistent with the one-electron reduction of an EPR-silent $[4Fe\text{-}4S]^{2+}$ species to a paramagnetic $[4Fe\text{-}4S]^{1+}$ cluster with electron spin $S =$, and exhibiting the fast spin relaxation typical of Fe-S clusters (Singh *et al.*, 2007). A brief description of the spectroscopy methods is included in the supplementary information (SI note 1). In sum, we demonstrate via anaerobic reconstitution and EDFS-EPR that *Mtb* WhiB4 contains a DTH-reducible 4Fe-4S cluster.

WhiB4 4Fe-4S cluster is responsive to O_2 and NO

Fe-S cluster proteins can function as global regulators by reacting with diatomic gases such as O_2 and NO (Green and Paget, 2004). To ascertain whether the WhiB4 4Fe-4S cluster is responsive to O_2, anaerobically reconstituted WhiB4 was exposed to air, and UV-visible spectra were recorded at various time points. After 5 min of exposure, we observed an increase in absorbance at 420 nm, followed by a gradual decline over the next 25 min, as well as a complete loss of protein color. At ~30 min post air exposure, the absorption spectrum was similar to that of the 2Fe-2S cluster originally present in the freshly purified WhiB4 protein (Fig. 2A). These spectral changes are consistent with an O_2-induced transformation of a [4Fe-4S] cluster to a [2Fe-2S] cluster (Singh *et al.*, 2007). Further incubation of air-exposed WhiB4 resulted in the complete loss of the cluster and the precipitation of the protein (data not shown). Analysis of the absorbance change at 420 nm versus time revealed the loss of ~80% of the 4Fe-4S cluster in 30 min. EDFS-EPR analysis of WhiB4 after brief air exposure (5 min) yielded an unresolved EPR spectrum with $g = 2.01$ (Fig. 2B). The shape and *g* value of the signal bears strong similarity to a $[3Fe\text{-}4S]^{1+}$ cluster, as observed with air-exposed FNR and WhiB3 proteins (Crack *et al.*, 2004, Singh *et al.*, 2007). This EPR signal was rapidly lost upon prolonged incubation (30 min) of air-exposed WhiB4 (Fig. 2B). Therefore, upon exposure to O_2, spectral features associated with the 4Fe-4S cluster were rapidly lost in a sequential reaction that yielded apo-WhiB4 via generation of $[3Fe\text{-}4S]^{1+}$ and [2Fe-2S] intermediates.

Next, to investigate whether NO can target the WhiB4 4Fe-4S cluster, anaerobically reconstituted WhiB4 was exposed to the fast NO-releasing compound proline NONOate (half-life 1.8 sec at pH 7.4) and analyzed with UV-visible spectroscopy and continuous

wave-EPR (cw-EPR). Exposure to NO leads to the formation of a new chromophoric species with a broad and intense near-UV absorption band at ~350 nm (Fig. 2C). This spectrum is similar to a dinitrosyl-iron dithiol complex (DNIC), wherein the sulfide ligands of the 4Fe-4S cluster are displaced by NO to form [Fe-$(NO)_2$] (Cruz-Ramos *et al.*, 2002). The EPR spectrum of anaerobically reconstituted, NO-exposed WhiB4 showed a strong EPR signal at $g = 2.03$ (Fig. 2D), suggesting the presence of a monomeric DNIC (Cruz-Ramos *et al.*, 2002). This spectrum was visible even at 200 K, indicating that this species was not an Fe-S cluster, whose rapid spin relaxation would preclude observation at such a high temperature. Taken together, these data demonstrate that the WhiB4 Fe-S cluster responds to O_2 and NO. An important discovery is that the 4Fe-4S cluster of WhiB4 is highly susceptible to O_2 damage, making it distinct from other WhiB-like proteins, such as WhiB3 and/or WhiB1, whose Fe-S clusters respond very slowly to O_2 exposure (Singh *et al.*, 2007, Smith *et al.*, 2010). These data suggest that WhiB4 can function as a sensor of redox signals via its 4Fe-4S cluster.

WhiB4 regulates growth, redox balance, and membrane potential *in vitro*

To understand the role of WhiB4 in the physiology of *Mtb*, we generated a *whiB4* mutant (*MtbΔwhiB4*) in *Mtb* via allelic exchange (Fig. S1A) and confirmed this disruption by PCR (Fig. S1B) and Southern blotting (Fig. S1C). A *whiB4* complemented strain (*comp.*) was also constructed (see *Experimental procedures*). Next, we examined the effect of WhiB4 disruption on the growth of *Mtb* in 7H9 liquid medium under normal aerobic conditions. We observed that *MtbΔwhiB4* cells consistently displayed a slow growth phenotype throughout the life cycle, which was marked by an ~2-fold reduction in colony forming units (CFU) as compared to wt *Mtb* (Fig. 3A). This result suggests that WhiB4 may play a role in maintaining an optimum overall growth of *Mtb*. We then examined the redox poise of NAD^+/NADH in *MtbΔwhiB4* during normal culture conditions (see *Experimental procedures*). Because NAD^+ and NADH are essential for shuttling electrons generated from the oxidation of carbon sources to the respiratory chain, the redox state of NAD^+/NADH is considered central to redox metabolism (Green and Paget, 2004). As shown in figure 3B, we consistently observed an ~2-fold reduced ratio of NAD^+/NADH in *MtbΔwhiB4* cells as compared to wt *Mtb* and the complemented strain throughout the growth cycle. This result implicates WhiB4 in regulating the redox steady state of the NAD^+/NADH couple, which contributes to proper growth of *Mtb* under *in vitro* conditions. Since the NAD^+/NADH redox state should be coupled to the electron transport chain, we analyzed the membrane potential (Ψ) of *MtbΔwhiB4* using the cationic fluorescent dye 3,3′-diethyloxacarbocyanine iodide ($DiOC_2$) as an indicator of respiration (see *Experimental procedures*). We observed an ~1.5-fold reduction in the value of Ψ in *MtbΔwhiB4* cells as compared to wt *Mtb* and the complemented strain (Fig. 3C). In sum, our data implicate WhiB4 in regulating oxidative metabolism and maintaining cellular redox homeostasis during normal aerobic growth of *Mtb*.

WhiB4 regulates the expression of antioxidant genes in *Mtb*

Next, we performed microarray analysis to examine the function of WhiB4 in *Mtb*. We compared the global transcription profile between wt *Mtb* and *MtbΔwhiB4* grown in 7H9 culture medium. Microarray data revealed that expression of only 26 genes was altered in *MtbΔwhiB4* under normal growing conditions. Of these 26 differentially regulated genes, expression of 25 was up-regulated by a factor of 1.3–2 in *MtbΔwhiB4*. To identify differentially expressed genes in *MtbΔwhiB4* that were of statistical significance, we performed SAM analysis (Significance Analysis of Microarray) as described in the *Experimental* procedures. The SAM results confirmed that 23 genes (Table S1) were indeed regulated by WhiB4 at the most stringent levels of analysis (false discovery rate= 0). Furthermore, we confirmed our microarray data by analyzing the expression of several

WhiB4-regulated genes via quantitative real-time PCR (qRT-PCR). The expression of these genes in wt *Mtb*, *MtbΔwhiB4*, and *whiB4* complemented strain was normalized against 16S rRNA expression levels (Table S2).

Consistent with the role of WhiB4 in sensing intracellular redox stress, expression data revealed that several genes associated with antioxidant systems were up-regulated in *MtbΔwhiB4*. Conventional antioxidant genes such as *ahpC* and *ahpD* encoding alkyl hydroperoxide reductase (Chen *et al.*, 1998) were induced in the mutant. A new discovery was the up-regulation of unconventional antioxidant systems in *MtbΔwhiB4*. For example, an operon-like cluster of four genes (Rv3249c-Rv3252c) encoding components of the rubredoxin system (*rubA, rubB*, and *alkB*) was also upregulated in *MtbΔwhiB4*. It has been shown that the rubredoxin system in bacteria (e.g., *Desulfovibrio vulgaris*) prevents auto-oxidation of redox enzymes and reduces intracellular levels of H_2O_2 and superoxide (Coulter and Kurtz, 2001). Another important inducible set of genes (Rv0692-Rv0694) shows similarity to enzyme complexes involved in the biosynthesis of the novel redox cofactor pyrroloquinoline quinone (PQQ) (Haft, 2011). PQQ is a powerful antioxidant that protects proteins and DNA from oxidative damage by scavenging ROI (Misra *et al.*, 2004). Microarray data revealed that the expression of *whiB4* was also induced in *MtbΔwhiB4*, suggesting an auto-repressor function of WhiB4. Presence of the initial 96 bases of the *whiB4* gene in *MtbΔwhiB4* likely facilitated the identification of the abortive *whiB4* transcript in these microarray experiments.

We observed that *whiB6* was also induced in *MtbΔwhiB4*. A recent comparison of all WhiB members demonstrates that *whiB6* expression exhibits the highest degree of stress-responsiveness (Geiman *et al.*, 2006). The up-regulation of *whiB6* in the absence of WhiB4 suggests that WhiB6 could be a compensatory mechanism for *Mtb* to sense and respond to intracellular redox stress. Finally, we show that several members of the PE-PPE family (PE35, PPE68, and PPE19) were also differentially regulated in *MtbΔwhiB4* (Table S1).

It is also noteworthy that there was a significant overlap between the genes regulated in *MtbΔwhiB4* and those differentially expressed in *Mtb* upon exposure to the anti-tuberculosis drug Isoniazid (INH). These include the components of the FASII operon involved in mycolic acid biosynthesis (Rv2243-Rv2246), the *iniBAC* operon, *ahpC-ahpD*, *nrdB,* Rv3250c-Rv3252c and *whiB4* (Betts *et al.*, 2003, Karakousis *et al.*, 2008). Peroxidative activation of INH by KatG is known to induce intracellular redox stress by generating endogenous ROI and RNI (Timmins and Deretic, 2006). Thus induction of INH-responsive genes in *MtbΔwhiB4* further implicates WhiB4 in sensing and maintaining endogenous redox balance. Taken together, our results suggest that WhiB4 regulates a specific set of genes involved in protecting *Mtb* from environmental stresses encountered during infection.

WhiB4 is a redox-dependent DNA binding protein

Having established that WhiB4 influences the expression of stress responsive genes in *Mtb*, we now sought to determine whether WhiB4 regulates gene expression by directly binding to DNA. To show this, we examined the interaction of WhiB4 with the promoter regions of *ahpC* and *whiB4*. We reconstituted the $[4Fe\text{-}4S]^{2+}$ form of WhiB4 (holo-WhiB4) under anaerobic conditions, which was confirmed via UV-visible spectroscopy as previously described. Reduced ($[4Fe\text{-}4S]^{1+}$) and oxidized ($[4Fe\text{-}4S]^{2+}$) holo-WhiB4 were assayed for DNA-binding activity under anaerobic conditions. We did not observe any noticeable DNA-binding activity of either reduced or oxidized holo-WhiB4 to either *ahpC* (Fig. S2) or *whiB4* promoter regions (data not shown).

Since WhiB4 rapidly loses its 4Fe-4S cluster upon air oxidation to generate apo-WhiB4, we determined whether degradation of the Fe-S cluster activated DNA binding of WhiB4. Apo-WhiB4 contains four Cys residues that have been shown to undergo thiol-oxidation or reduction in response to diamide or DTT, respectively (Alam *et al.*, 2009). In the presence of diamide, apo-WhiB4 binds to the promoter regions of *ahpC* and *whiB4* in a concentration-dependent manner (Fig. 4A and 4C). In contrast, DNA binding by apo-WhiB4 was completely lost in the presence of DTT (Fig. 4B and 4D). Lastly, we independently replaced the four Cys residues in WhiB4 with alanine and analyzed the DNA binding capacity of mutant proteins using *ahpC* promoter. The absence of DNA binding in the case of Cys mutants suggests that the oxidation of four Cys residues is essential for the DNA binding activity of apo-WhiB4 (Fig. S3). These results demonstrate that DNA binding of apo-WhiB4 is regulated by the redox state of the Cys residues and suggest that O_2-activated Fe-S cluster degradation and subsequent oxidation of Cys thiols serve as a switch to activate WhiB4 for its role in gene regulation.

WhiB4 binds DNA in a sequence independent manner

We next tested whether apo-WhiB4 binds DNA specifically or non-specifically by competition assays. Since *ahpC* was identified as one of the genes regulated by WhiB4, we used its promoter DNA fragment to examine whether binding was specific, while a non-related promoter fragment of a *Mtb* gene (Rv3849, *espR*) was utilized as a negative control. We found that a 50-fold molar excess of the unlabeled *ahpC* promoter fragment completely prevented binding of oxidized apo-WhiB4 to the labeled *ahpC* promoter (Fig. 4E). However, the same concentrations of an unlabelled *espR* promoter fragment also reduced apo-WhiB4 binding to approximately similar extent, suggesting non-specific DNA binding activity of apo-WhiB4 (Fig. 4F). The sequence-independent DNA binding of the oxidized apo-WhiB4 was further analyzed by examining its interaction with the unrelated promoter fragments derived from *Mtb* genes *pks3* (Rv1180) and *rrnA*. As shown in figure S4, apo-WhiB4 displayed efficient binding to both the promoters.

To gain the mechanistic understanding of WhiB4 non-specific DNA binding activity, we further extended our study on the regulation of *ahpC* expression by WhiB4. The expression of *ahpC* is controlled via OxyR in other mycobacterial species such as *M. leprae* and *M. avium*. In *M. leprae*, OxyR binds to its consensus sequence in the *ahpC* promoter (Pagan-Ramos *et al.*, 1998), whereas in *Mtb*, both the *oxyR* ORF and its consensus sequence in the *ahpC* promoter region contain multiple mutations (Pagan-Ramos *et al.*, 1998). We addressed whether WhiB4 could discriminate between the OxyR binding motif present in the promoter sequences of *ahpC* from *Mtb* and *M. leprae*. To do this, we performed DNA binding assays using an ~40bp oligonucleotide containing *Mtb* or *M. leprae* OxyR binding sequence. Our data demonstrated that apo-WhiB4 binds to the fragment containing the *Mtb* OxyR binding motif in a concentration dependent manner with a dissociation constant (K_d) of approximately 1 μM (Fig. 5A). In contrast, we found that apo-WhiB4 binding to the *M. leprae* fragment was significantly reduced (~10% of the *M. leprae* as compared to ~60% of the *Mtb ahpC* promoter fragment was bound at 1 μM of apo-WhiB4) (Fig. 5B). These results indicate that WhiB4 prefers OxyR binding sequence in the promoter of *Mtb ahpC* over *M. leprae ahpC*.

Mtb WhiB4 preferentially binds to GC-rich sequences

Since WhiB4 binds to the *Mtb ahpC* promoter region, we used this region to search for consensus sequences in the promoter regions of other genes regulated by WhiB4. We found no consensus patterns upon alignment of the sequences ~400 bp upstream of the start codon for the genes regulated by WhiB4. However, closer inspection of the OxyR consensus sequence in the *ahpC* promoter region revealed that it is relatively GC-rich (56%) in *Mtb* as

compared to *M. leprae* (30%). The upstream sequences (~400bp) from the other 23 WhiB4 regulated genes showed that they were also GC-rich (56–70%). This indicates that WhiB4 could bind DNA non-specifically with a preference for GC-rich sequences.

To examine this possibility, we randomly modified the GC content of the OxyR binding motif in the *Mtb ahpC* promoter. Figure 5C lists the mutations tested in this experiment. First, we confirmed that apo-WhiB4 binding to the 40 bp *Mtb ahpC* promoter fragment can be efficiently outcompeted by the non-specific promoter regions of *Mtb espR* (58% GC) and *cfp10* (60% GC) (Fig. S5). Next, DNA binding was performed using randomly modified fragments of varying GC content and oxidized apo-WhiB4. Figure 5D shows that apo-WhiB4 binds with the wt *Mtb ahpC* promoter (56% GC). However, DNA binding was significantly reduced in the case of mutant promoters M1 and M2 with a GC content of 32 and 44%, respectively (Fig. 5D). Furthermore, DNA binding was fully restored when the GC content was increased to 68 and 85% in the M3 and M4 fragments, respectively (Fig. 5D). Kinetic analysis confirmed that apo-WhiB4 binds to the M3 and M4 fragments with K_d values of 0.6 and 0.4 μM, respectively (Fig S6). These findings were separately verified by competition assays using wt *ahpC*, M1, M2, M3 and M4 fragments. Figure 5E demonstrates that competition with a 50-fold molar excess of specific wt *ahpC* promoter (56% GC) resulted in complete loss of DNA binding, whereas the same concentration of either M1 (32% GC) or M2 (44% GC) resulted in a modest loss of WhiB4 DNA binding. In contrast, we observed that only a 10-fold molar excess of M3 (68% GC) and M4 (85% GC) fragments was required to completely abolish WhiB4 DNA binding (Fig. 5E).

Lastly, we found that WhiB4 DNA binding to the wt *ahpC* promoter was efficiently competed by excessive poly (dG:dC) and poly (dI:dC) but not by poly (dA:dT) (Fig. S7). In sum, data generated suggest that WhiB4 is a non-specific DNA binding protein with a preference for GC-rich DNA sequences.

DNA minor groove binding drugs compete with WhiB4 for DNA binding

Since AT- and GC-rich sequences are known to influence groove topology in DNA (Rohs *et al.*, 2009), we evaluated the ability of major and minor groove binding drugs to compete against WhiB4:DNA interactions. We used actinomycin D and chromomycin A3, as minor groove binding drugs, and methyl green, a major groove binding drug in our competition assays. As shown in figure S7, actinomycin D and chromomycin A3 effectively abolished binding of WhiB4 to the *ahpC* promoter fragment, whereas methyl green had no effect. These results suggest that WhiB4 binds to GC-rich DNA through the minor groove. The ability of minor groove binding proteins to regulate expression by remodeling DNA architecture (Bewley *et al.*, 1998) suggests that WhiB4 could repress expression of stress genes by binding in the minor groove of GC-rich promoters and changing the conformation of the promoter regions.

Apo-WhiB4 represses transcription *in vitro*

To understand the influence of apo-WhiB4 DNA binding on transcription, we performed *in vitro* transcription assays using a highly sensitive *Mycobacterium smegmatis* (*Msm*) RNA polymerase holoenzyme containing stoichiometric concentrations of the principal sigma factor, SigA (RNAP-σ^A) (See SI note 2). The *Msm* RNAP-σ^A specifically binds to and activates transcription from the σ^A -dependent promoters (China and Nagaraja, 2010). To identify which of the WhiB4-regulated genes are recognized and transcribed by RNAP-σ^A, we performed single round transcription assays using the promoter regions of *ahpC*, *iniB*, and *whiB4*. The *rrnA* promoter was used as a positive control forσ^A -specific transcription. In these assays, RNAP-σ^A transcription activity was not detected at the *ahpC* or *iniB* promoters (data not shown). However, RNAP-σ^A catalyzes transcription specifically from

whiB4 and *rrnA* promoters, producing a single major transcript of ~260 bp and ~210 bp, respectively (Fig. 6A and B). The size of *rrnA* transcript is in agreement with the reported transcriptional start point (TSP) for the *rrnA* ORF (Verma *et al.*, 1994, Gonzalez-y-Merchand *et al.*, 1996), confirming the specificity of RNAP-σ^A activity (see SI note 3). In silico promoter analysis of *whiB4* using Artificial Neural Networks Promoter Prediction tool (ANNPP 2.2, http://www.fruitfly.org/seq_tools/~promoter.html) program (Kalate *et al.*, 2003) revealed the presence of a putative -10 like sequence and a potential TSP, which corresponds to the size of the *whiB4* transcript detected in our assays (see SI note 3). Next, we assessed the influence of apo-WhiB4 on the transcription from *whiB4* and *rrnA* promoters. Addition of oxidized apo-WhiB4 completely inhibited transcription from the *whiB4* and *rrnA* promoters, whereas reduced apo-WhiB4 restored the transcription to normal levels (Fig. 6A and B). These data demonstrate that WhiB4 affects transcription in a redox-dependent, but promoter-sequence-independent manner. The non-specific DNA binding and transcriptional inhibition exhibited by WhiB4 is mechanistically similar to several nucleoid associated proteins (NAPs) in bacteria (Colangeli *et al.*, 2007, Dillon and Dorman, 2010).

Apo-WhiB4 oligomerizes *in vitro* and *in vivo*

To examine the oligomeric status of oxidized and reduced apo-WhiB4, we performed non-reducing western blot analysis of apo-WhiB4 using anti-His antibody. Western blot analysis of air-oxidized apo-WhiB4 yielded three bands of ~14 kDa, ~28 kDa, and ~42 kDa that correspond to the size of a full length His-tagged apo-WhiB4 monomer, dimer, and trimer, respectively (Fig. 6C). In contrast, the oligomeric apo-WhiB4 forms were gradually reduced to monomeric form by increasing amounts of β-mercaptoethanol (β-ME) (Fig. 6C). The presence of SDS resistant oligomers under non-reducing conditions indicates the formation of intermolecular disulfide bonds between the Cys thiols of apo-WhiB4.

To determine whether the formation of disulfide bonded oligomers might be of physiological significance, we used an anhydrotetracycline (ATc) inducible *E.coli-mycobacterial* shuttle plasmid pEXCF-*whiB4* containing FLAG-tagged *whiB4*. The pEXCF-*whiB4* was electroporated in *Msm* and WhiB4 was conditionally expressed using ATc as described in the *Experimental procedures*. The presence of WhiB4 was detected in the cell free extract of *Msm* by non-reducing western blot analysis using anti-FLAG antibody. In the absence of ATc, we detected a faint band of apo-WhiB4 migrated as a trimer, indicating the presence of disulfide-linked oligomers (Fig. 6D). Furthermore, over-expression of WhiB4 by ATc demonstrates that apo-WhiB4 mainly exists as a trimer (Fig. 6D). To conclusively determine that disulfide-linked oligomers existed in the intact cells and were not generated during cell extract preparation, we pretreated *Msm* expressing FLAG-tagged WhiB4 with the membrane permeable alkylating agent, N-ethylmaleimide (NEM) as described in the *Experimental procedures*. NEM alkylates free-SH groups, blocking their participation in disulfide bond formation, but does not disrupt the existing disulfide bonds. As shown in figure 6D, a significant portion (~90%) of apo-WhiB4 exists as a trimer, whereas only a fraction of apo-WhiB4 is present in a reduced monomer form under alkylating conditions in the intact cells. Furthermore, DTT-reduction of the NEM treated samples converted a major fraction of the oligomeric apo-WhiB4 to the monomeric form (Fig. 6D). These data show that apo-WhiB4 oligomerizes via intermolecular disulfide bonds inside aerobically growing *Msm*, suggest that some trimeric apo-WhiB4 could be disulfide linked in *Mtb* cells to bind DNA and repress transcription.

WhiB4 regulates the survival of *Mtb* upon oxidative stress

Having shown that WhiB4 modulates the expression of genes involved in dissipating oxidative stress, we analyzed the sensitivity of *MtbΔwhiB4* to ROI generators such as CHP

and menadione. We found that *MtbΔwhiB4* survived 20-fold better than wt *Mtb* upon exposure to 25 and 50 μM of CHP (Fig. S8A). Consistent with this, *MtbΔwhiB4* also displayed 10-fold better survival against 40–50 μM menadione compared to wt *Mtb* (Fig. S8B). This resistance phenotype was reversed in the *whiB4* complemented strain (Fig. S8A and S8B). These observations suggest that the increased resistance of *MtbΔwhiB4* to oxidative stress could be due to the induction of antioxidant systems in the mutant.

WhiB4 modulates the induction of antioxidant genes upon oxidative stress

Here we examine whether WhiB4 regulates the expression of antioxidants gene in response to oxidative stress. We exposed wt *Mtb* and *MtbΔwhiB4* to CHP and analyzed the expression by qRT-PCR. Exposure to CHP resulted in the induction of *ahpC*, *ahpD*, *rubA*, *pqqE*, Rv3249c, and *whiB6* in wt *Mtb* as compared to unstressed cells (Table S3). However, the expression of these genes was consistently higher in the CHP treated *MtbΔwhiB4* as compared to wt *Mtb* (Table S3). Furthermore, we detected a significant down-regulation of *whiB4* in the CHP treated wt *Mtb*, whereas the expression of partial *whiB4* transcript was moderately induced in the CHP treated *MtbΔwhiB4* (Table S3). The effect of CHP on the expression was restored to near wt *Mtb* levels in the *whiB4* complemented strain. In sum, our data suggest that WhiB4 modulates the ability of *Mtb* to resist oxidative stress by the controlled activation of antioxidant response.

WhiB4 modulates survival of *Mtb* during infection of macrophages

Given that WhiB4 regulates expression of antioxidant genes, resulting in differential survival of *Mtb* in response to oxidative stress *in vitro*, and that *Mtb* encounters oxidative stress during infection, we hypothesize that WhiB4 protein plays an important role in the infection process. To test this hypothesis, we performed a series of experiments with cultured cells and whole animal systems, comparing the performance of *MtbΔwhiB4* to wt Mtb.

Infection of macrophages exposes *Mtb* to oxidative and nitrosative stresses (Gordon and Read, 2002). Therefore, we first examined the phenotype of *MtbΔwhiB4* in resting Raw264.7 macrophages. *MtbΔwhiB4* grew at a level similar to wt *Mtb* inside resting macrophages (Fig. S9). Since macrophages activated by IFN-γ and LPS generate a more hostile environment by inducing vacuole acidification, nutrient depletion, and enhanced ROI/RNI production to constrain bacterial growth (James *et al.*, 1995, Schaible *et al.*, 1998), we analyzed the influence of the activation status of the infected macrophages on the survival of *MtbΔwhiB4*. In activated macrophages, we observed an ~50-fold enhanced survival of *MtbΔwhiB4* as compared to wt *Mtb* at day 2 post-infection (Fig. 7A). This difference was further amplified to ~1,000-fold at day 4 post-infection (Fig. 7A). The original survival phenotype of *MtbΔwhiB4* was significantly restored in the complemented strain. This trend was confirmed in three independent experiments.

Until now, we have shown the effect of WhiB4 in controlling *Mtb* survival inside murine macrophages cultivated at ambient O_2 pressure (20%; pO_2 140 mm Hg). However, 20% O_2 is not physiologically relevant because human tissues maintain O_2 levels of 5% (36 mm Hg) (Meylan *et al.*, 1992a, Meylan *et al.*, 1992b). Interestingly, it has been shown that human monocytes displayed higher ROI production and effectively controlled the replication of *Mtb* when cultured at 5% O_2 (Meylan *et al.*, 1992b). To investigate the role of WhiB4 in settings closer to physiological conditions, we examined the survival of *MtbΔwhiB4* in THP-1 human monocytic cell lines cultivated at 20% (ambient) and 5% (reduced) O_2 levels. As shown in Figure 7B and 7C, wt *Mtb* grew normally at higher O_2 tension (20%), whereas lower pO_2 consistently reduced its growth at early time points, followed by a slow increase in the survival. This intracellular growth pattern of wt *Mtb* at 5% O_2 was in agreement with

the original study reported by Meylan *et al.* (Meylan *et al.*, 1992b). In contrast, *MtbΔwhiB4* grew more robustly than wt *Mtb* inside THP-1 macrophages at both 20% and 5% O_2 (Fig. 7B and 7C), at all time points of infection, with the most striking difference at low O_2 tension (5%) (Fig. 7C). Lastly, at both O_2 concentrations, the growth phenotype of the complemented strain was restored to wild- type levels (Fig. 7B and 7C). This phenotype of *MtbΔwhiB4* was confirmed in three independent experiments. Taken together, the data generated from *in vitro* and macrophage experiments clearly suggest that WhiB4 functions as a sensor of oxidative stress and modulates the survival of *Mtb* in response to enhanced antimycobacterial activity in macrophages.

WhiB4 regulates *Mtb* persistence and dissemination *in vivo*

Till date, there has been only one study showing the importance of a WhiB protein (WhiB3) in regulating the pathogenesis of *Mtb* in animal models (Steyn *et al.*, 2002). The observation that WhiB4 modulates oxidative stress survival prompted us to investigate the effect of this protein during infection in guinea pigs. Aerosol infection of outbred Hartley guinea pigs showed a clear growth benefit of *MtbΔwhiB4* as compared to wt *Mtb* in the lungs of animals. Results show that nearly identical numbers of bacteria were seeded in the lungs of animals infected with various strains at day 1 post-infection (Fig. 8A). At day 30 post-infection, the number of bacteria present in the lungs of *MtbΔwhiB4* infected guinea pigs was ~6-fold higher ($P<0.001$) than those infected with wt *Mtb* (Fig. 8A). Importantly, guinea pigs were able to control wt *Mtb* growth following activation of the adaptive immune response (~45 days post-infection). At this time, the bacillary load of *MtbΔwhiB4* was ~8-fold higher than wt *Mtb* (Fig. 8A). Interestingly, and in contrast to our lung data, bacterial number in the spleen at 30 and 45-days post-infection was lesser for *MtbΔwhiB4* than the wt *Mtb* ($P<0.001$), suggesting that WhiB4 is necessary for dissemination and/or colonization of *Mtb* to the spleen (Fig. 8B). Finally, the *in vivo* phenotype of *MtbΔwhiB4* was abolished in case of animals infected with the *whiB4* complemented strain (Fig. 8A and 8B).

Mtb WhiB4 regulates pathogenesis in guinea pigs

To further investigate the unique phenotype exhibited by *MtbΔwhiB4 in vivo*, we performed a histopathological analysis of parts of the lungs and spleen from infected animals. We did not observe a significant difference in the number of granulomas present in the lung lesions of animals infected with either wt *Mtb* or *MtbΔwhiB4*. However, the pulmonic lesions of *MtbΔwhiB4* infected animals showed larger and more necrotic granulomas as compared to animals infected with wt *Mtb* or complemented strain at 30 and 45 days post-infection (Fig. 8C, 8D, 8E and S10), suggesting severe pathological changes induced by the mutant.

The spleen of wt *Mtb* infected guinea pigs displayed larger granulomas with well delineated central necrotic areas at 30 days post-infection (Fig. 8C). In contrast, the splenic parenchyma of *MtbΔwhiB4* infected animals displayed no evidence of organized granulomas (Fig. 8D). At 45 days post-infection, the splenic lesions in *MtbΔwhiB4* infected animals showed the presence of granulomas with modest necrosis, however, the pathology remained less severe as compared to wt *Mtb* infected spleen (Fig. S10). These data suggest that the high load of *MtbΔwhiB4* induces severe lung pathology, whereas its delayed dissemination results in slow progression of spleen pathology.

Taken together, these results reveal a previously unidentified phenotype of *Mtb in vivo* and suggest that WhiB4 is important for regulating survival in the lungs and dissemination of pathogen to the extrapulmonary tissues.

Discussion

In the present work, we provide a new mechanistic insight into the molecular function of WhiB4 in *Mtb* and demonstrate that WhiB4 binds DNA and regulates the expression of antioxidant and stress responsive genes in *Mtb*. Our data suggest that WhiB4 is a part of a system that carefully controls the expression of antioxidant genes in *Mtb* to modulate survival and dissemination *in vivo*.

Mtb WhiB4 contains a redox responsive $[4Fe\text{-}4S]^{2+}$ cluster, which degrades within minutes of exposure to O_2. The presence of extremely O_2-labile 4Fe-4S cluster was not reported in other WhiB family members (Jakimowicz *et al.*, 2005, Singh et al., 2007, Smith *et al.*, 2010), suggesting that differences in the redox potential of Fe-S clusters may control the function of WhiB proteins. As is the case for FNR and SoxR (Green and Paget, 2004), NO also targets the WhiB4 Fe-S cluster, suggesting that WhiB4 activity can be modulated by nitrosylation of its Fe-S cluster during infection. Our results are in agreement with an earlier report showing the presence of a 4Fe-4S cluster in WhiB4 (Alam *et al.*, 2007). However, the redox state and the O_2/NO reaction intermediates of the WhiB4 4Fe-4S cluster remained uncharacterized. Our study provides biochemical characterization of redox, O_2, and NO sensing properties of the Fe-S cluster in WhiB4. Biochemical and expression data suggest that WhiB4 maintains redox homeostasis by regulating the expression of oxidative stress response systems in *Mtb*. We found that almost all of the WhiB4 repressed genes were differentially expressed under stress condition(s) that mimic the *in vivo* environment. For example, *ahpC-ahpD* is activated in response to ROI, RNI, and inside activated macrophages (Schnappinger *et al.*, 2003). Similarly, *rubA*, *rubB, and alkB* were found to be differentially regulated under acidic pH, hypoxic conditions, starvation, and inside macrophages (Betts *et al.*, 2002, Schnappinger *et al.*, 2003, Kim *et al.*, 2008). Expression of *icl, nrdB, iniB, kasA, kasB, acpM, fabD, whiB4 and whib6* is regulated by a wide variety of stress conditions such as acidic pH, drug treatment (INH/ETH), oxidative stress, detergent (SDS), and heat stress (Fisher *et al.*, 2002, Betts *et al.*, 2003, Schnappinger *et al.*, 2003, Geiman *et al.*, 2006). To explore the underlying mechanism of WhiB4 function, we characterized its redox and DNA binding properties and found that the loss of Fe-S cluster and the subsequent oxidation of the coordinating Cys thiols stimulate WhiB4 DNA binding and transcriptional repression. Furthermore, oxidation of Cys thiols stimulates intermolecular disulfide bond formation between apo-WhiB4 monomer in a DTT-reversible manner. In addition, we detected the presence of disulfide-linked endogenous oligomers of apo-WhiB4 in *Msm* over-expressing FLAG-tagged WhiB4. Taken together, these findings suggest that the formation of stabilized oligomeric apo-WhiB4 by one or more disulfide bonds may be the regulatory mechanism that controls WhiB4 DNA binding and transcriptional activity.

Our result indicating the presence of disulfide-linked apo-WhiB4 inside the reduced environment of mycobacterial cytosol is not unprecedented. In *Rhodobacter capsulatus*, CrtJ (a DNA binding repressor) and RegB (a sensor kinase) contain redox-active Cys residues that exist in a disulfide bonded form during aerobic culturing conditions (Masuda *et al.*, 2002, Swem *et al.*, 2003). Moreover, Cys residues flanked by basic amino acids are known to have a significantly lower *pKa*, leading to deprotonation of their sulfhydryl group at physiological pH. Interestingly, WhiB4 contains several cationic amino acids that surround the Cys residues (Lys36-Cys37-Arg38, Cys59-Arg60), which may decrease Cys residues *pKa*, resulting in the formation of Cys thiolates and disulfide bonds in the cytosol of mycobacteria.

Although, metal-based sensors (e.g., SoxR, IscR, FNR) require redox-active Fe-S cluster for DNA binding and transcription (Green and Paget, 2004), recent studies involving *E.coli*

IscR, *B. cereus* FNR, *Mtb* WhiB3, and *Mtb* WhiB1 have identified a mechanism analogous to WhiB4, in which the loss of Fe-S and redox-modifications of Cys thiols activate their role in gene regulation (Esbelin *et al.*, 2008, Nesbit *et al.*, 2009, Singh *et al.*, 2009, Smith *et al.*, 2010). While the *in vitro* data suggest that disulfide bond formation may be responsible for the redox-sensing and DNA binding activity of WhiB4, it cannot be discounted that other Fe-S cluster intermediates (*e.g.* 3Fe-4S, 2Fe-2S) or oxidized Cys derivatives (e.g., sulfenic acid) may be occurring inside *Mtb* cells that affect the activity of WhiB4.

The specificity of *Mtb* WhiB proteins for DNA binding is not fully understood. It has been previously shown that apo-WhiB3 binds DNA with a low degree of sequence discrimination (Singh *et al.*, 2009), which is consistent with a genome-wide study showing the lack of a consensus motif for the WhiB3 DNA binding (Guo *et al.*, 2009). Similarly, apo-WhiB1 binds to a large region of promoter DNA rather than a core motif, suggesting a flexible DNA binding specificity (Smith *et al.*, 2010). Although, apo-WhiB2 DNA binding is shown to be specific for the *whiB2* promoter (Rybniker *et al.*, 2010), a methodical study examining the effect of the redox state of holo- and apo-WhiB2 on DNA binding remains uncharacterized. We show that apo-WhiB4 binds to DNA non-specifically with a preference for GC-rich sequences, interacts with the minor groove of DNA, and represses transcription. While, our *in vitro* data suggest that WhiB4 functions as a non-specific DNA binding repressor, further experiments are needed to conclusively demonstrate the transcriptional regulatory properties of WhiB4 *in vivo*. .Nonetheless, the aforementioned characteristics along with a low molecular weight (13.1 kDa) and a highly basic pI (pI = 10.28) of WhiB4 are reminiscent of nucleoid associated proteins (NAPs) such as HNS, HU, and Lsr2 (Colangeli *et al.*, 2007, Dillon and Dorman, 2010). The NAPs are promiscuous in their interaction with DNA, but show preference towards AT-rich sequences and minor groove (Dillon and Dorman, 2010). Interestingly, *Mtb* NAP Lsr2, binds to the upstream regions of *whiB4* and other WhiB4-regulated genes (e.g. *iniB*, *ahpC*, *icl*, etc.), suggesting a potential overlapping role for Lsr2 and WhiB4 in gene expression. However, in contrast to WhiB4, Lsr2 binds *Mtb* DNA with a preference for the AT-rich sequences (AT content ~47%) (Gordon *et al.*, 2011). The preference of WhiB4 for DNA fragments with a GC content equivalent to the average *Mtb* genome (*i.e.* ~65%) suggests a large number of binding sites in the *Mtb* genome, which is contrary to the modest effect of WhiB4 loss on the gene expression. This could simply be due to low endogenous levels of oxidized apo-WhiB4 under the conditions tested. Alternatively, apo-WhiB4 may interact with one or more regulatory proteins (e.g., WhiB6, Rv3249c, Lsr2) that either counter-balance the effect of WhiB4 loss or provide sequence-specificity to its DNA binding. Since expression of WhiB4 is induced by nutrient limitation (Betts *et al.*, 2002) and enduring hypoxia (Rustad *et al.*, 2008), it may well be that under these conditions WhiB4 changes transcriptional pattern by interacting non-specifically with the nucleoid (currently in progress).

The association between oxidative stress and WhiB4 was further substantiated by our data showing repression of *whiB4* in response to CHP treatment and the reported down-regulation of *whiB4* expression inside the infected macrophages (Rachman *et al.*, 2006). It seems that the regulation of transcription orchestrated by WhiB4 occurs at two levels in response to oxidative stress. Under mild oxidizing conditions (e.g., resting macrophages), sequential degradation of WhiB4 4Fe-4S cluster and subsequent generation of disulfide-linked apo-WhiB4 oligomers result in the transcription repression of stress genes. *Mtb* further regulates the activity of apo-WhiB4 by systematically reducing *whiB4* expression via WhiB4 and/or Lsr2 in response to a gradual increase in oxidative stress (e.g., activated macrophages). This down-regulation of WhiB4 can steadily reduce its control on gene expression, necessary for the calibrated derepression of antioxidant and stress genes to avoid excessive virulence for long term persistence of *Mtb*.

Although our *in vitro* CHP experiment cannot mimic the complexity of redox environment encountered by *Mtb in vivo*, it is tempting to speculate that the uncontrolled expression of antioxidant and stress genes may be partly responsible for the enhanced survival of *MtbΔwhiB4* in macrophages and hypervirulence in the lungs of guinea pigs. Complementation studies confirm that phenotypes are WhiB4-specific. However, contribution of other regulatory factors which are either over-expressed in *MtbΔwhiB4* (WhiB6 and Rv3249c) or modulate *whiB4* expression (Lsr2), should also be examined to fully understand the *in vivo* phenotype of *MtbΔwhiB4* and is the subject of future investigation.

An unexpected observation in this study is that *whiB4* is essential for successful dissemination and/or colonization of *Mtb* in spleen. This finding is difficult to reconcile with the hypervirulence of *MtbΔwhiB4* in the lungs of guinea pigs, unless extrapulmonary dissemination and pulmonary persistence are interrelated. Consistent with this view, it has been shown that dissemination of *Mtb* to extrapulmonary organs precedes the induction of the adaptive immune response in the infected host (Chackerian *et al.*, 2002). This suggests that hypervirulence of *MtbΔwhiB4* in the lungs may also be the consequence of weaker stimulation of the protective host response in the spleen due to delayed dissemination of the mutant to the splenic tissues. Alternatively, differences in the environment of spleen and lungs (e.g., O_2 tension) may have accounted for the tissue-specific phenotype of *MtbΔwhiB4*.

Taken together, our data implicate WhiB4 in regulating oxidative stress response to modulate the virulence of *Mtb*. However, the precise role of WhiB4 in controlling gene expression, dissemination, and immune modulation is complex and is a focus of an independent study.

Ethics Statement

This study was carried out in strict accordance with the guidelines provided by the Committee For The Purpose Of Control and Supervision on Experiments on Animals (CPCSEA), Government of India. The protocol was approved by the Committee on the Ethics of Animal Experiments of the International Centre for Genetic Engineering and Biotechnology, New Delhi, India (Approval number: ICGEB/AH/2011/2/IMM-26). All efforts were made to minimize the suffering.

Experimental Procedures

Bacterial Strains and Growth Conditions

Mtb H37Rv, *MtbΔwhiB4*, and *Mtb whiB4* complemented strains were grown aerobically in inkwell bottles with shaking (150 rpm) at 37°C in 7H9 broth (Difco) or 7H11 agar (Difco) supplemented with 0.2% glycerol, Middlebrook albumin-dextrose-catalase (ADC) enrichment and 0.1 % Tween 80 (broth). *E. coli* cultures were grown in LB medium. Antibiotics were added as described earlier (Singh *et al.*, 2007).

Overexpression and purification of WhiB4

The recombinant WhiB4 was purified as N-terminal His-tagged recombinant protein. The entire ORF of *Mtb whiB4* (Rv3681c) was PCR amplified from *Mtb* H37Rv genomic DNA using gene-specific oligonucleotides pCOLD*whiB4F* and pCOLD*whiB4R* (Table S4). The amplicon was digested with *Bam*HI and *Hind*III, and ligated into similarly digested His-tag based expression vector, pCOLD1 (TAKARA BIO INC, Clontech Laboratories, CA, USA). The resulting plasmid, pCOLD-WhiB4, was then transformed into *E. coli* BL21 (DE3) strain and WhiB4 protein was purified to homogeneity at 15°C by using a His-tag based affinity

purification, as described previously (Singh *et al.*, 2009). The *whiB4* gene on pCOLD-WhiB4 was mutated using oligonucleotide based site-directed mutagenesis approach (Xu *et al.*, 1996) to create individual cysteine to alanine substitutions. Sequences of oligonucleotides used to create mutations are shown in table S4. Resulting clones were verified by sequencing, and the mutant Cys variants of the wild type WhiB4 were purified as described earlier.

Fe-S cluster assembly

WhiB4 Fe-S cluster reconstitution was performed under anoxic conditions, monitored by UV-vis spectroscopy, and analyzed by EPR analysis as described (See SI Experimental procedures).

EPR spectroscopy

The EDFS EPR measurements were made on an ELEXSYS-E 680 spectrometer (Bruker, Billerica, MA) equipped with an electrically controlled Oxford liquid He transfer line attached to a rectangular type cryostat. EDFS EPR spectra were measured with a two-pulse echo sequence ($\pi/2$ - t - π - t - echo). Typically, microwave pulse lengths (tMW) of 16 and 32 ns were used with t = 180 ns. NO-treated WhiB4 was analyzed by cw EPR on a perpendicular mode X-band EPR spectrometer operating at 100-kHz modulation frequency and equipped with liquid helium cryostat (Oxford Instruments, Oxon, U.K.) and a dual mode X-band cavity (Bruker ERA116DM). Field calibration was done by using a standard NMR G meter. EPR was performed at the Department of Biochemistry, University of Alabama at Tuscaloosa, USA.

Construction of *MtbΔwhiB4*

The allelic replacement of *whiB4* was carried out as described (Bardarov *et al.*, 2002). A detailed description is provided in the supplementary information (SI Experimental procedures).

In vitro growth assays

For CHP stress assays, bacteria were grown in 7H9 broth to mid-log phase (OD_{600} of 0.3) and exposed to 25 and 50 μM of CHP (Sigma-Aldrich) for 24 hrs followed by plating for CFU analysis. For menadione stress assays, bacteria were grown in 7H9 broth at 37°C till mid-log phase (OD_{600} of 0.3) and 10-fold serial dilutions were plated on 7H11 plates containing 0, 20, 40, and 50 μM of menadione (Sigma-Aldrich). The plates were incubated at 37°C for 3–4 weeks and colonies were counted to measure percent survival.

Estimation of NAD^+/NADH and detection of membrane potential

Various strains of *Mtb* were grown in 7H9 medium and subjected to NAD^+/NADH analysis as previously described (Singh *et al.*, 2009). See SI Experimental procedures.

Microarray hybridization and data analysis

For microarray analysis, the total RNA was extracted from the three biological replicates of aerobically cultured wild type *Mtb* H37Rv and *MtbΔwhiB4* at an OD_{600} of 0.4 as described (Singh *et al.*, 2009). Microarrays were produced, processed and analyzed at the Center for Applied Genomics at the Public Health Research Institute, New Jersey (See SI Experimental procedures).

qRT-PCR

Mtb cells were grown till an OD_{600} of 0.4 and RNA was isolated as described (Singh *et al.*, 2009). For analyzing the influence of CHP on the expression, *Mtb* cells were grown till an OD_{600} of 0.4 and treated with 1 mM of CHP for 1.5 h. This was followed by total RNA isolation and qRT-PCR analysis as described (see SI Experimental procedures).

Preparation of redox modified forms of WhiB4

The redox modified forms of holo-WhiB4 and apo-WhiB4 for the DNA binding reactions were generated as described (see SI Experimental procedures).

EMSA analysis

For EMSA assays, the promoter fragments (~300-350 bp upstream of the translational start codon) of *ahpC*, *whiB4, pks3, rrnA, espR* were PCR amplified from the *Mtb* H37Rv genome and the 5'-end was labeled with [γ-^{32}P] ATP (Perkin Elmer) using T4 polynucleotide kinase (MBI Fermentas) according to the manufacturer's instructions. For EMSA analysis with the OxyR binding site in the promoter region of *ahpC*, various oligonucleotides (40 bp) containing *Mtb* and *M. leprae oxyR* binding sites were synthesized as shown in figure 7C. Binding reactions were performed in buffer containing 89 mM Tris, 89 mM boric acid and 1 mM EDTA, pH 8.4 in the presence of 0.50 ng poly dI:dC. The reactions were separated using 4–20% gradient TBE PAGE gels (Bio-Rad). Gels were exposed to autoradiographic film and visualized via phosphorimaging (GE).

In vitro transcription assays

The DNA templates including the putative *whiB4* promoter regions and *rrn*A promoter were prepared by PCR using primers P*whiB4* F1/P*whiB4* R1 and P*rrnA*F1/P*rrnA*R1, respectively (Table S4). The amplicons (50 nM) were pre-incubated with apo-WhiB4 in the transcription buffer (50 mM Tris-HCl, 3 mM of magnesium acetate, 0.1 mM DTT, 5% glycerol, 50 μg/ml BSA and 50 mM KCl) for 30 min at room temperature. Single-round transcription reactions were initiated with the addition of 50 nM of RNAP-σ^A, 100 μM of NTPs, 1 μCi [α-^{32}P] UTP, 50 μg/ml heparin and allowed to proceed at 37°C for 15 min. The reactions were terminated by formamide gel loading dye and then transcripts were resolved on a 10% TBE-urea-PAGE gel (Bio-Rad).

Construction of the *Msm* strain carrying FLAG-tagged WhiB4

The entire ORF of *whiB4* was PCR amplified from *Mtb* H37Rv genomic DNA with primers BP-*whiB4F* and BP-*whiB4R*. The PCR product was then cloned downstream of tetracycline responsive *tetRO* regulatory sequences in an *E.coli*-mycobacterial shuttle vector pEXCF to generate pEXCF-*whiB4* using GATEWAY™ Cloning Technology (Invitrogen) as per manufacturer's instructions. The C-terminus of *whiB4* ORF was cloned in frame with the FLAG-tag sequence present in the pEXCF vector. The pEXCF-*whiB4* was then electroporated into *Msm* and transformants were selected on hygromycin. The expression of FLAG-tagged WhiB4 was induced by adding 200 ng/ml anhydrotetracycline (Cayman chemicals) to the logarithmically grown *Msm* cultures for 4h at 37°C.

Non-reducing western blot analysis

The apo- form of aerobically purified WhiB4 was generated as described earlier. The apo-WhiB4 was either exposed to atmospheric O_2 or treated with β-ME and resolved by 12% non-reducing SDS-PAGE. Proteins were transferred on to 0.2 μm PVDF membrane and used for Western blot. Western blot analysis was achieved using 1:4000 dilution of anti-His antibody (Qiagen) for 12 h. The blotted membrane was developed with a 1:4000 dilution of

peroxidase-conjugated anti-mouse IgG (Cell signaling) and an enhanced chemiluminescence substrate (GE Amersham).

Msm WhiB4 FLAG-tag strain was grown aerobically in flask shaking at 200 r.p.m till an OD_{600} of 0.5, induced with 200 ng/ml of ATc for 4hr at 37°C, and pelleted. Pellets were resuspended in lysis buffer (300mM NaCl, 20mM Na-Phosphate, 10% Glycerol and protease inhibitor, pH 7.5) and sonicated. Sample (30 μg) was added to non-reducing loading dye and separated by non-reducing SDS-PAGE. Proteins were transferred on to a 0.2 μm PVDF membrane and used for Western blot. Western blot analysis was achieved using 1:4000 dilution of anti-FLAG antibody (Sigma-Aldrich) for 12 h and blots were developed as described earlier. For NEM experiment, *Msm* WhiB4 FLAG-tag cells were harvested and suspended in the lysis buffer containing 10 mM of NEM for 10 min followed by sonication and non-reducing Western blot analysis.

Survival of *MtbΔwhiB4* in macrophages

Raw 264.7 macrophages were either non-activated or activated with rIFN-γ (50 U ml^{-1}) and LPS (10 ng) for 16h. Various strains of *Mtb* were added at a multiplicity of infection of 10 to triplicate wells, incubated for 4 hr, washed, and resuspended in gentamycin-containing fresh DMEM medium. Samples were collected at 0, 2, and 4 days, post-infection by lysing infected cells with 0.1% SDS. Lysates were diluted in PBS/Tween and plated on 7H10 agar. Colonies were counted after 3–4 weeks at 37°C. Infection of THP-1 human monocytic cell lines was performed as described previously (Kumar *et al.*, 2010). Infected cells were cultivated at 5% O_2 concentration (pO_2 36 mm Hg) in a humidified incubator (New Brunswick Scientific) and processed for CFU analysis at 0, 2, and 4 days post-infection as described earlier.

Aerosol infection of guinea pigs

Outbred Hartley guinea pigs (~300–400 g body weight) (National Institute of Nutrition, Hyderabad, India) were given a low dose of *Mtb* using a Madison chamber aerosol generation instrument calibrated to deliver 50–100 CFU. Animals were sacrificed (n=5) at 1, 30 and 45 days post-infection for determination of organ bacterial burden and histopathology analysis. The statistical significance of the differences between experimental groups was determined by two-tailed, unpaired student's *t*-test. Differences with a P value of <0.05 were considered significant.

Histopathology analysis was performed as described previously (Singh *et al.*, 2003). Briefly, sections of lungs and spleen were fixed in 10% neutral buffered formalin for embedding in paraffin, sectioning and staining with hematoxylin and eosin. A blinded examination of at least three serial sections from each guinea pig was carried out to evaluate the number of granulomas, inflammation, degree of necrosis, and mixed cells infiltrate.

Supplementary Material

Refer to Web version on PubMed Central for supplementary material.

Acknowledgments

We thank V. Nagaraja (IISc, Bangalore, India) for *Msm* RNAP-σ^A holoenzyme and David R. Sherman (Seattle Biomed, USA) for pEXCF-*whiB4* construct. This work was supported by the Wellcome-DBT India Alliance grant, WTA01/10/355 (AS) and in part by the following NIH grants: a developmental supplement to P30AI027767 (AS) from the NIH Office of AIDS Research (OAR) entitled Creative and Novel Ideas in HIV Research (CNIHR) and NIAID grants AI058131 (AJCS), AI068928 (AJCS). This work was also supported by a Department of Biotechnology (DBT) grants DB01/11/413 (AS) and DB01/10/363 (DK). AS is a Wellcome-DBT India Alliance Intermediate Fellow We gratefully acknowledge DBT-India for providing Tuberculosis Aerosol Challenge Facility

(TACF) at ICGEB for guinea pigs studies. We thank Santosh Kumar for excellent technical help in facilitating the animal experiments.

References

Alam MS, Garg SK, Agrawal P. Molecular function of WhiB4/Rv 3681c of *Mycobacterium tuberculosis* H37Rv: a [4Fe-4S] cluster co-ordinating protein disulphide reductase. Mol Microbiol. 2007; 63:1414–1431. [PubMed: 17302817]

Alam MS, Garg SK, Agrawal P. Studies on structural and functional divergence among seven WhiB proteins of *Mycobacterium tuberculosis* H37Rv. Febs J. 2009; 276:76–93. [PubMed: 19016840]

Bardarov S, Bardarov S Jr, Pavelka MS Jr, Sambandamurthy V, Larsen M, Tufariello, et al. Specialized transduction: an efficient method for generating marked and unmarked targeted gene disruptions in *Mycobacterium tuberculosis*, *M. bovis* BCG and *M. smegmatis*. Microbiology. 2002; 148:3007–3017. [PubMed: 12368434]

Betts JC, Lukey PT, Robb LC, McAdam RA, Duncan K. Evaluation of a nutrient starvation model of *Mycobacterium tuberculosis* persistence by gene and protein expression profiling. Mol Microbiol. 2002; 43:717–731. [PubMed: 11929527]

Betts JC, McLaren A, Lennon MG, Kelly FM, Lukey PT, Blakemore SJ, Duncan K. Signature gene expression profiles discriminate between isoniazid-, thiolactomycin-, and triclosan-treated *Mycobacterium tuberculosis*. Antimicrob Agents Chemotherap. 2003; 47:2903–2913.

Bewley CA, Gronenborn AM, Clore GM. Minor groove-binding architectural proteins: structure, function, and DNA recognition. Annu Rev Biophys Biomol Struct. 1998; 27:105–131. [PubMed: 9646864]

Chackerian AA, Alt JM, Perera TV, Dascher CC, Behar SM. Dissemination of *Mycobacterium tuberculosis* is influenced by host factors and precedes the initiation of T-cell immunity. Infect Immun. 2002; 70:4501–4509. [PubMed: 12117962]

Chen L, Xie QW, Nathan C. Alkyl hydroperoxide reductase subunit C (AhpC) protects bacterial and human cells against reactive nitrogen intermediates. Mol Cell. 1998; 1:795–805. [PubMed: 9660963]

China A, Nagaraja V. Purification of RNA polymerase from mycobacteria for optimized promoter-polymerase interactions. Protein Expr Purif. 2010; 69:235–242. [PubMed: 19815074]

Colangeli R, Helb D, Vilcheze C, Hazbon MH, Lee CG, Safi H, et al. Transcriptional regulation of multi-drug tolerance and antibiotic-induced responses by the histone-like protein Lsr2 in *M. tuberculosis*. PLoS Pathog. 2007; 3:e87. [PubMed: 17590082]

Cooper AM, Segal BH, Frank AA, Holland SM, Orme IM. Transient loss of resistance to pulmonary tuberculosis in $p47^{phox-/-}$ mice. Infect Immun. 2000; 68:1231–1234. [PubMed: 10678931]

Coulter ED, Kurtz DM Jr. A role for rubredoxin in oxidative stress protection in *Desulfovibrio vulgaris*: catalytic electron transfer to rubrerythrin and two-iron superoxide reductase. Arch Biochem Biophys. 2001; 394:76–86. [PubMed: 11566030]

Crack J, Green J, Thomson AJ. Mechanism of oxygen sensing by the bacterial transcription factor fumarate-nitrate reduction (FNR). J Biol Chem. 2004; 279:9278–9286. [PubMed: 14645253]

Cruz-Ramos H, Crack J, Wu G, Hughes MN, Scott C, Thomson AJ, et al. NO sensing by FNR: regulation of the *Escherichia coli* NO-detoxifying flavohaemoglobin, Hmp. EMBO J. 2002; 21:3235–3244. [PubMed: 12093725]

den Hengst CD, Buttner MJ. Redox control in actinobacteria. Biochim Biophys Acta. 2008; 1780:1201–1216. [PubMed: 18252205]

Deretic V, Philipp W, Dhandayuthapani S, Mudd MH, Curcic R, Garbe T, et al. *Mycobacterium tuberculosis* is a natural mutant with an inactivated oxidative-stress regulatory gene: implications for sensitivity to isoniazid. Mol Microbiol. 1995; 17:889–900. [PubMed: 8596438]

Dillon SC, Dorman CJ. Bacterial nucleoid-associated proteins, nucleoid structure and gene expression. Nat Rev Microbiol. 2010; 8:185–195. [PubMed: 20140026]

Esbelin J, Jouanneau Y, Armengaud J, Duport C. ApoFnr binds as a monomer to promoters regulating the expression of enterotoxin genes of *Bacillus cereus*. J Bacteriol. 2008; 190:4242–4251. [PubMed: 18424517]

Farhana A, Guidry L, Srivastava A, Singh A, Hondalus MK, Steyn AJ. Reductive Stress in Microbes: Implications for Understanding *Mycobacterium tuberculosis* Disease and Persistence. Adv Microb Physiol. 2010; 57:43–117. [PubMed: 21078441]

Fisher MA, Plikaytis BB, Shinnick TM. Microarray analysis of the *Mycobacterium tuberculosis* transcriptional response to the acidic conditions found in phagosomes. J Bacteriol. 2002; 184:4025–4032. [PubMed: 12081975]

Geiman DE, Raghunand TR, Agarwal N, Bishai WR. Differential gene expression in response to exposure to antimycobacterial agents and other stress conditions among seven *Mycobacterium tuberculosis* whiB-like genes. Antimicrob Agents Chemother. 2006; 50:2836–2841. [PubMed: 16870781]

Gonzalez-y-Merchand JA, Colston MJ, Cox RA. The rRNA operons of *Mycobacterium smegmatis* and *Mycobacterium tuberculosis*: comparison of promoter elements and of neighbouring upstream genes. Microbiology. 1996; 142 (Pt 3):667–674. [PubMed: 8868442]

Gordon BR, Li Y, Cote A, Weirauch MT, Ding P, Hughes TR, et al. Structural basis for recognition of AT-rich DNA by unrelated xenogeneic silencing proteins. Proc Natl Acad Sci USA. 2011; 108:10690–10695. [PubMed: 21673140]

Gordon SB, Read RC. Macrophage defences against respiratory tract infections. Br Med Bull. 2002; 61:45–61. [PubMed: 11997298]

Green J, Paget MS. Bacterial redox sensors. Nat Rev Microbiol. 2004; 2:954–966. [PubMed: 15550941]

Guo M, Feng H, Zhang J, Wang W, Wang Y, Li Y, et al. Dissecting transcription regulatory pathways through a new bacterial one-hybrid reporter system. Genome Res. 2009; 19:1301–1308. [PubMed: 19228590]

Haft DH. Bioinformatic evidence for a widely distributed, ribosomally produced electron carrier precursor, its maturation proteins, and its nicotinoprotein redox partners. BMC Genomics. 2011; 12:21. [PubMed: 21223593]

Jakimowicz P, Cheesman MR, Bishai WR, Chater KF, Thomson AJ, Buttner MJ. Evidence that the *Streptomyces* developmental protein WhiD, a member of the WhiB family, binds a [4Fe-4S] cluster. J Biol Chem. 2005; 280:8309–8315. [PubMed: 15615709]

James PE, Grinberg OY, Michaels G, Swartz HM. Intraphagosomal oxygen in stimulated macrophages. J Cell Physiol. 1995; 163:241–247. [PubMed: 7706368]

Kalate RN, Tambe SS, Kulkarni BD. Artificial neural networks for prediction of mycobacterial promoter sequences. Comput Biol Chem. 2003; 27:555–564. [PubMed: 14667783]

Karakousis PC, Williams EP, Bishai WR. Altered expression of isoniazid-regulated genes in drug-treated dormant *Mycobacterium tuberculosis*. J Antimicrob Chemother. 2008; 61:323–331. [PubMed: 18156607]

Khoroshilova N, Popescu C, Munck E, Beinert H, Kiley PJ. Iron-sulfur cluster disassembly in the FNR protein of *Escherichia coli* by O_2: [4Fe-4S] to [2Fe-2S] conversion with loss of biological activity. Proc Natl Acad Sci USA. 1997; 94:6087–6092. [PubMed: 9177174]

Kim SY, Lee BS, Shin SJ, Kim HJ, Park JK. Differentially expressed genes in *Mycobacterium tuberculosis* H37Rv under mild acidic and hypoxic conditions. J Med Microbiol. 2008; 57:1473–1480. [PubMed: 19018016]

Kumar D, Nath L, Kamal MA, Varshney A, Jain A, Singh S, Rao KV. Genome-wide analysis of the host intracellular network that regulates survival of *Mycobacterium tuberculosis*. Cell. 2010; 140:731–743. [PubMed: 20211141]

Lee PP, Chan KW, Jiang L, Chen T, Li C, Lee TL, et al. Susceptibility to mycobacterial infections in children with X-linked chronic granulomatous disease: a review of 17 patients living in a region endemic for tuberculosis. The Pediatr Infect Dis J. 2008; 27:224–230.

MacMicking JD, North RJ, LaCourse R, Mudgett JS, Shah SK, Nathan CF. Identification of nitric oxide synthase as a protective locus against tuberculosis. Proc Natl Acad Sci USA. 1997; 94:5243–5248. [PubMed: 9144222]

Masuda S, Dong C, Swem D, Setterdahl AT, Knaff DB, Bauer CE. Repression of photosynthesis gene expression by formation of a disulfide bond in CrtJ. Proc Natl Acad Sci USA. 2002; 99:7078–7083. [PubMed: 11983865]

Meylan PR, Richman DD, Kornbluth RS. Oxygen tensions and mycobacterial infections. Clin Infect Dis. 1992a; 15:372–373. [PubMed: 1520772]

Meylan PR, Richman DD, Kornbluth RS. Reduced intracellular growth of mycobacteria in human macrophages cultivated at physiologic oxygen pressure. Am Rev Respir Dis. 1992b; 145:947–953. [PubMed: 1554224]

Misra HS, Khairnar NP, Barik A, Indira Priyadarsini K, Mohan H, Apte SK. Pyrroloquinoline-quinone: a reactive oxygen species scavenger in bacteria. FEBS Lett. 2004; 578:26–30. [PubMed: 15581610]

Nesbit AD, Giel JL, Rose JC, Kiley PJ. Sequence-specific binding to a subset of IscR-regulated promoters does not require IscR Fe-S cluster ligation. J Mol Biol. 2009; 387:28–41. [PubMed: 19361432]

Ng VH, Cox JS, Sousa AO, MacMicking JD, McKinney JD. Role of KatG catalase-peroxidase in mycobacterial pathogenesis: countering the phagocyte oxidative burst. Mol Microbiol. 2004; 52:1291–1302. [PubMed: 15165233]

Pagan-Ramos E, Song J, McFalone M, Mudd MH, Deretic V. Oxidative stress response and characterization of the *oxyR-ahpC* and *furA-katG* loci in *Mycobacterium marinum.* J Bacteriol. 1998; 180:4856–4864. [PubMed: 9733688]

Rachman H, Strong M, Schaible U, Schuchhardt J, Hagens K, Mollenkopf H, et al. *Mycobacterium tuberculosis* gene expression profiling within the context of protein networks. Microbes Infect. 2006; 8:747–757. [PubMed: 16513384]

Rohs R, West SM, Sosinsky A, Liu P, Mann RS, Honig B. The role of DNA shape in protein-DNA recognition. Nature. 2009; 461:1248–1253. [PubMed: 19865164]

Rustad TR, Harrell MI, Liao R, Sherman DR. The enduring hypoxic response of *Mycobacterium tuberculosis*. PloS One. 2008; 3:e1502. [PubMed: 18231589]

Rybniker J, Nowag A, van Gumpel E, Nissen N, Robinson N, Plum G, Hartmann P. Insights into the function of the WhiB-like protein of mycobacteriophage TM4 - a transcriptional inhibitor of WhiB2. Mol Microbiol. 2010; 77:642–657. [PubMed: 20545868]

Schaible UE, Sturgill-Koszycki S, Schlesinger PH, Russell DG. Cytokine activation leads to acidification and increases maturation of *Mycobacterium avium*-containing phagosomes in murine macrophages. J Immunol. 1998; 160:1290–1296. [PubMed: 9570546]

Schnappinger D, Ehrt S, Voskuil MI, Liu Y, Mangan JA, Monahan IM, et al. Transcriptional Adaptation of *Mycobacterium tuberculosis* within Macrophages: Insights into the Phagosomal Environment. J Exp Med. 2003; 198:693–704. [PubMed: 12953091]

Singh A, Crossman DK, Mai D, Guidry L, Voskuil MI, Renfrow MB, Steyn AJ. *Mycobacterium tuberculosis* WhiB3 maintains redox homeostasis by regulating virulence lipid anabolism to modulate macrophage response. PLoS Pathog. 2009; 5:e1000545. [PubMed: 19680450]

Singh A, Guidry L, Narasimhulu KV, Mai D, Trombley J, Redding KE, et al. *Mycobacterium tuberculosis* WhiB3 responds to O2 and nitric oxide via its [4Fe-4S] cluster and is essential for nutrient starvation survival. Proc Natl Acad Sci USA. 2007; 104:11562–11567. [PubMed: 17609386]

Singh R, Rao V, Shakila H, Gupta R, Khera A, Dhar N, et al. Disruption of *mptpB* impairs the ability of *Mycobacterium tuberculosis* to survive in guinea pigs. Mol Microbiol. 2003; 50:751–762. [PubMed: 14617138]

Smith LJ, Stapleton MR, Fullstone GJ, Crack JC, Thomson AJ, Le Brun NE, et al. *Mycobacterium tuberculosis* WhiB1 is an essential DNA-binding protein with a nitric oxide-sensitive iron-sulfur cluster. Biochem J. 2010; 432:417–427. [PubMed: 20929442]

Steyn AJC, Collins DM, Hondalus MK, Jacobs WR Jr, Kawakami RP, Bloom BR. *Mycobacterium tuberculosis* WhiB3 interacts with RpoV to affect host survival but is dispensable for in vivo growth. Proc Natl Acad Sci USA. 2002; 99:3147–3152. [PubMed: 11880648]

Swem LR, Kraft BJ, Swem DL, Setterdahl AT, Masuda S, Knaff DB, et al. Signal transduction by the global regulator RegB is mediated by a redox-active cysteine. EMBO J. 2003; 22:4699–4708. [PubMed: 12970182]

Ta DT, Vickery LE. Cloning, sequencing, and overexpression of a [2Fe-2S] ferredoxin gene from *Escherichia coli*. J Biol Chem. 1992; 267:11120–11125. [PubMed: 1317854]

Timmins GS, Deretic V. Mechanisms of action of isoniazid. Mol Microbiol. 2006; 62:1220–1227. [PubMed: 17074073]

Verma A, Kinger AK, Tyagi JS. Functional analysis of transcription of the *Mycobacterium tuberculosis* 16S rDNA-encoding gene. Gene. 1994; 148:113–118. [PubMed: 7926824]

Xu X, Kang SH, Heidenreich O, Li Q, Nerenberg M. Rapid PCR method for site-directed mutagenesis on double-stranded plasmid DNA. Biotechniques. 1996; 20:44–47. [PubMed: 8770404]

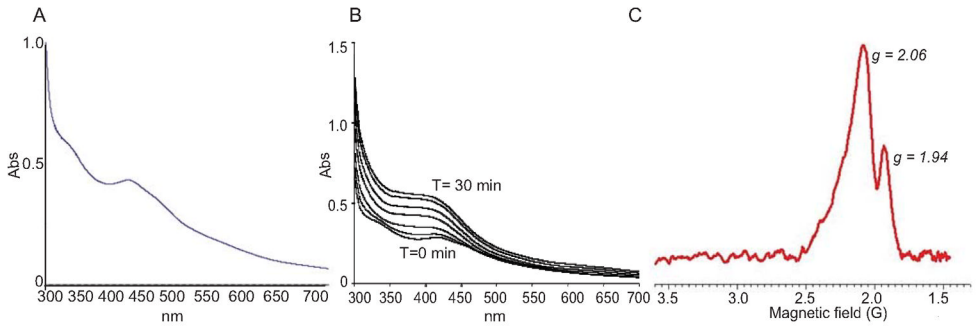

Fig. 1. Spectroscopic characterization of WhiB4

(A) Aerobically purified WhiB4 was scanned by a UV-vis spectrophotometer. Note the presence of broad peaks at ~330 nm, ~ 420, and ~450 nm characteristic of a 2Fe-2S cluster. (B) UV-visible spectra of anaerobically reconstituted WhiB4. Enzymatic reconstitution of WhiB4 Fe-S was carried out inside an anaerobic glove box. Note the time dependent increase in the characteristic 4Fe-4S cluster peak at 420 nm. Reconstitution of the 4Fe-4S cluster was completed in 30 min. (C) EDFS-EPR spectra of reconstituted WhiB4 after reduction with sodium dithionite (DTH). The experimental conditions were: $\pi/2$ and π pulses of 16 and 32 ns; τ = 180 ns; T = 9K. Spectra were acquired 60 shots with a two-step cycle at a repetition rate of 1 kHz. Microwave frequency = 9.806 GHz.

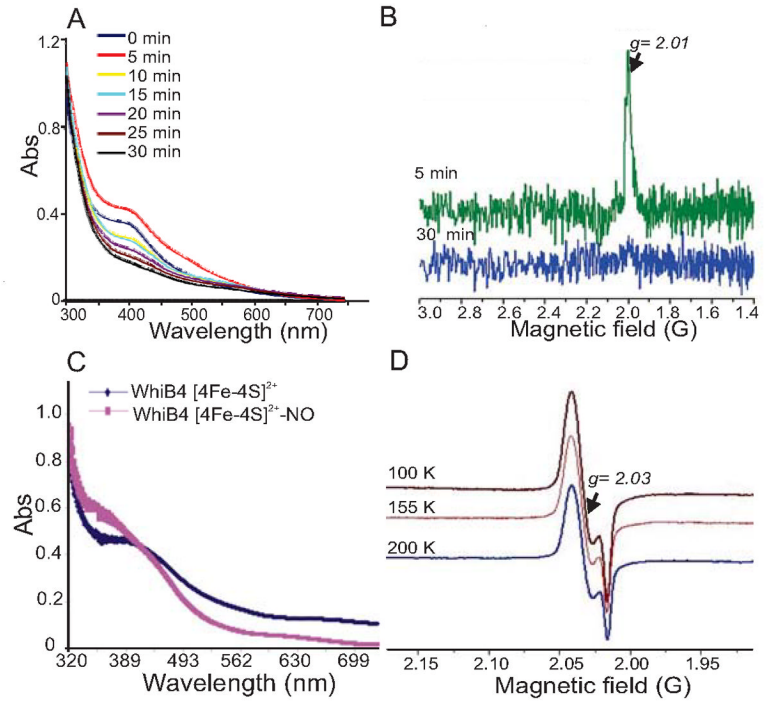

Fig. 2. The *Mtb* WhiB4 Fe-S cluster responds to O_2 and NO

(A) UV-visible spectra were obtained before and after exposing anaerobically reconstituted WhiB4 4Fe-4S cluster to air at various time points. Note the time dependent decrease in the absorbance at 420 nm. (B) Air-exposed samples of reconstituted WhiB4 were withdrawn immediately (5 min; green spectrum) or 30 min post-exposure (blue spectrum) and analyzed by EDFS-EPR. The appearance of a sharp signal at $g = 2.01$ indicates a $[3Fe\text{-}4S]^{1+}$ cluster. Conditions for EPR spectroscopy were the same as in figure 1(C). The influence of NO on WhiB4 was analyzed by adding a 10-fold molar excess of proline NONOate (WhiB4:NO) before analysis by UV-visible and cw-EPR spectroscopy. (C) UV-visible spectra were acquired before and after addition of proline NONOate. Note the increase in the characteristic monomeric DNIC peak at ~350 nm in the NO treated sample. (D) cw-EPR spectra of NO treated samples were acquired at a microwave frequency of 9.667 GHz and microwave power of 2 mW at 100, 155, and 200 K. The appearance of a sharp signal around 2.03 and the increase in the intensity of the signal at lower temperatures is consistent with the formation of monomeric DNIC.

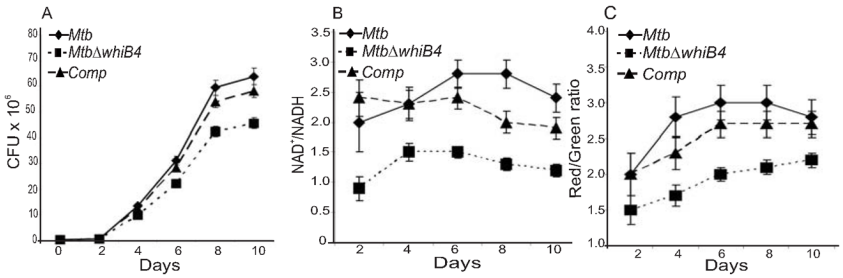

Fig. 3. WhiB4 modulates growth, redox homeostasis, and membrane potential of *Mtb* under aerobic conditions

(A) Aerobic growth phenotype of wt *Mtb*, *MtbΔwhiB4*, and complemented strains was determined by growing cells in 7H9 medium under aerobic conditions. Growth was monitored at different time intervals by CFU analysis. (B) At various days post-inoculation, cells were analyzed for intracellular redox balance by measuring the poise of NAD^+/NADH as described in the *Experimental procedures*. (C) Membrane potential of aerobically growing cells was determined by staining with $DiOC_2$. A change in the membrane potential was detected using the average mean fluorescence intensity (Red/Green) emitted by the cells. The fluorescent intensity was normalized to the values obtained upon carbonyl cyanide *m*-chlorophenyl hydrazone (CCCP) treatment. All of the above experiments were carried out at least three times in triplicate and results are given as the mean values and standard deviations.

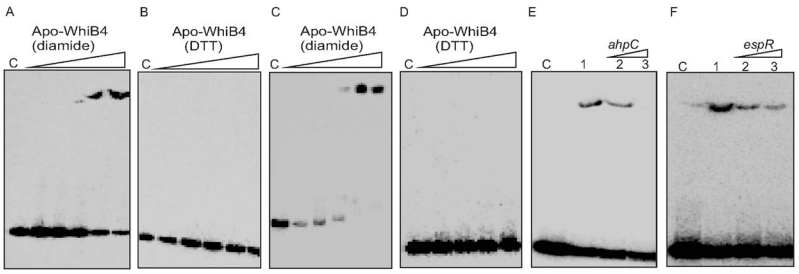

Fig. 4. DNA binding activity of WhiB4

Apo-WhiB4 was prepared as described in the *Experimental procedures*. The concentrations of apo-WhiB4 used for EMSAs were 0.1, 0.2, 0.4, 0.8 and 1 μM. EMSA reactions were performed with 0.2 nM of γ-^{32}P labeled *ahpC* (A and B) and *whiB4* (C and D) promoter DNA fragments. DNA binding of apo-WhiB4 in the presence of thiol-oxidant, diamide (A and C) or thiol-reductant, DTT (B and D). C: DNA binding in the absence of WhiB4 in each panel. (E and F) Sequence preference of WhiB4 for DNA binding. EMSAs were performed using γ-^{32}Plabeled *ahpC* promoter DNA with 800 nM of apo-WhiB4 in the presence of 50 mM diamide. The DNA binding was competed using increasing concentrations of unlabeled *ahpC* (specific) or *espR* (non-specific) promoter DNA. Lane 1 in panel E and F: WhiB4:*ahpC* promoter complex. WhiB4 DNA binding was competed using 10-fold (lane 2) and 50-fold (lane 3) molar excess of either unlabeled *ahpC* (E) or *espR* (F) promoter DNA. C: DNA binding in the absence of WhiB4 in each panel.

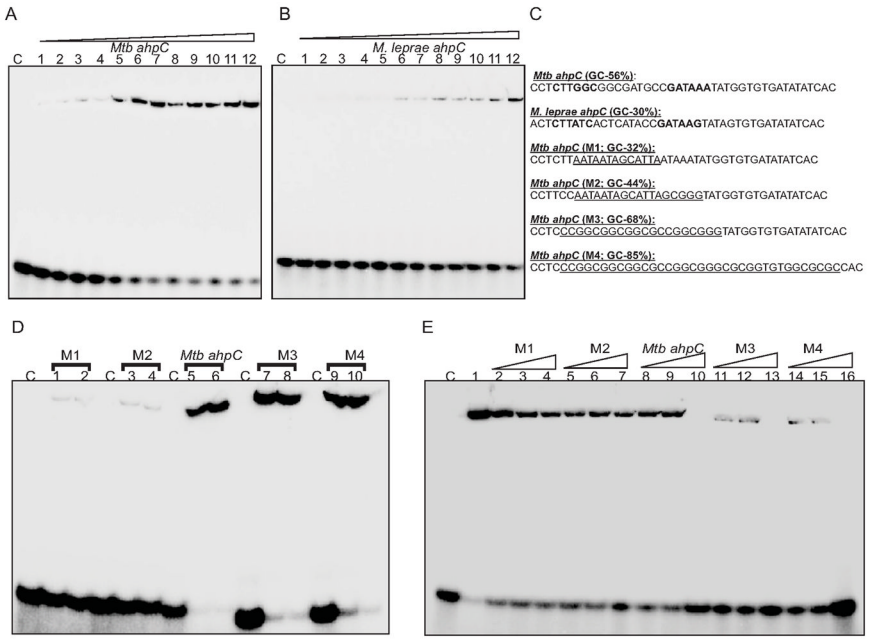

Fig. 5. WhiB4 binds to GC-rich DNA

Concentration dependent binding of oxidized apo-WhiB4 to a 40 bp γ-^{32}P labeled DNA fragment derived from (A) *Mtb* and (B) *M. leprae ahpC* promoter regions containing the OxyR binding motif. The concentrations of oxidized apo-WhiB4 were 0.25, 0.50, 0.75, 1.00, 1.25, 1.50, 1.75, 2.0, 2.25, 2.50, 2.75, 3.00 μM. The K_d for both the fragments was calculated by measuring the intensity of free and protein bound DNA using ImageJ software. Note that apo-WhiB4 binds with higher affinity to the GC-rich *Mtb* OxyR recognition sequence as compared to the AT-rich *M. leprae* OxyR recognition sequence within the *ahpC* promoter. (C) DNA fragments containing mutations to modify the GC content of the *ahpC* promoter region (OxyR binding core motif is shown in bold). The mutated sequences in various DNA fragments (M1–M4) are underlined. These fragments were subjected to EMSA analysis. (D) EMSAs were carried out using 0.8 and 1 μM of oxidized apo-WhiB4 and 0.2 nM of γ-^{32}P labeled DNA fragments. Note that apo-WhiB4 showed enhanced binding to M3 (68% GC) and M4 (85% GC) as compared to M1 (32% GC) and M2 (44% GC) fragments. (E) Competition assay using high and low GC DNA fragments. Lane 1: oxidized apo-WhiB4:*ahpC* promoter complex. DNA binding was competed using 10-fold (lanes 2,5,8,11,and 14), 20-fold (lanes 3,6,9,12, and 15), and 50-fold (lanes 4,7,10,13, and 16) molar excess of unlabeled DNA fragments as indicated in the figure. C: DNA binding in the absence of WhiB4 in each panel.

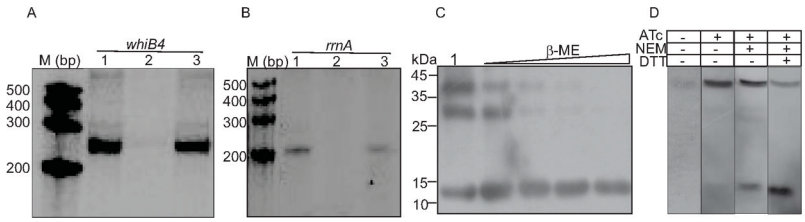

Fig. 6. (A and B) Effect of WhiB4 on *in vitro* transcription

Single round transcription assays show that RNAP-σ^A holoenzyme was proficient in directing transcription from *whiB4* (panel A; lane 1) and *rrnA* (panel B; lane 1) promoters. 50 nM of *whiB4* and *rrnA* promoter DNA fragments were pre-incubated with either 2 μM oxidized apo-WhiB4 (panel A; lane 2 and panel B; lane 2) or reduced apo-WhiB4 (panel A; lane 3 and panel B; lane 3) and subjected to transcription by RNAP-σ^A. M: RNA marker (Century™ Marker Template, Ambion). **(C) Disulfide bond formation induces oligomerization of apo-WhiB4 *in vitro***. 5 μg of apo-WhiB4 is either oxidized by atmospheric O_2 (lane 1) or reduced by 50 mM,100 mM, 200 mM, and 400 mM of β-ME and resolved on a 12% non-reducing SDS-PAGE. Apo-WhiB4 bands were visualized by western blot analysis using anti-His antibody. The ~14 kDa, ~28 kDa, and ~42 kDa bands correspond to the His-tagged apo-WhiB4-monomer, -dimer and –trimer. **(D) *In vivo* existence of disulfide-linked oligomers of apo-WhiB4**. Aerobically grown *Msm* WhiB4 FLAG-tag strain was either uninduced or induced with ATc and 30 μg of cell free extract was analyzed by non-reducing western blot using anti-FLAG antibody. Note that a significant portion of the FLAG-tagged apo-WhiB4 exists as a trimer in ATc induced *Msm* cells. To minimize the possibility of O_2-induced thiol-oxidation and subsequent oligomerization of apo-WhiB4 during cell free extract preparation, *Msm* cells expressing FLAG-tagged WhiB4 were pretreated with the thiol-alkylating agent NEM. Note the presence of apo-WhiB4 trimer in the NEM pretreated sample. A significant loss of apo-WhiB4 oligomerization upon DTT reduction further suggests the presence of intermolecular disulfide-linked oligomers *in vivo*.

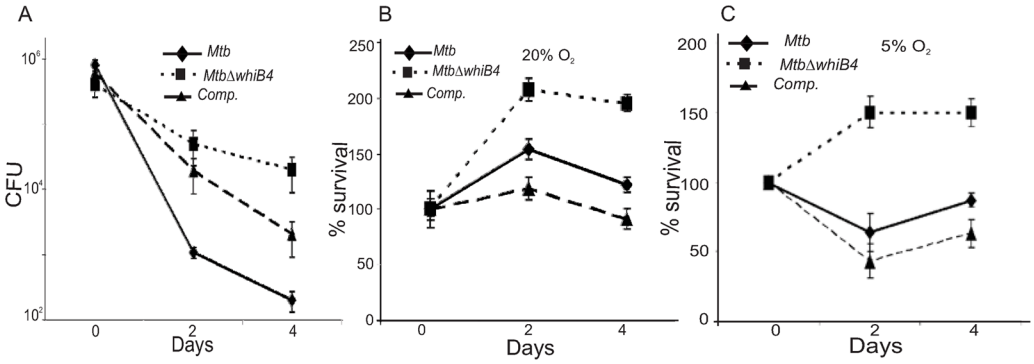

Fig. 7. WhiB4 regulates survival of *Mtb* inside macrophages

(A) rIFNγ and LPS activated Raw264.7 cells were infected with *Mtb* strains at a MOI of 10 and growth was monitored over time by CFU. To investigate the role of O_2 tension, phorbol 12-myristate 13-acetate (PMA) stimulated THP-1 human monocytic cell lines were maintained at 20% O_2 (B) and 5% O_2 (C) and infected by various *Mtb* strains at a MOI of 10. For each strain, the CFU at each time point are expressed relative to the CFU at time 0. In each case, data shown is the average of three experiments performed in triplicate; the error bars indicate standard deviation in each group.

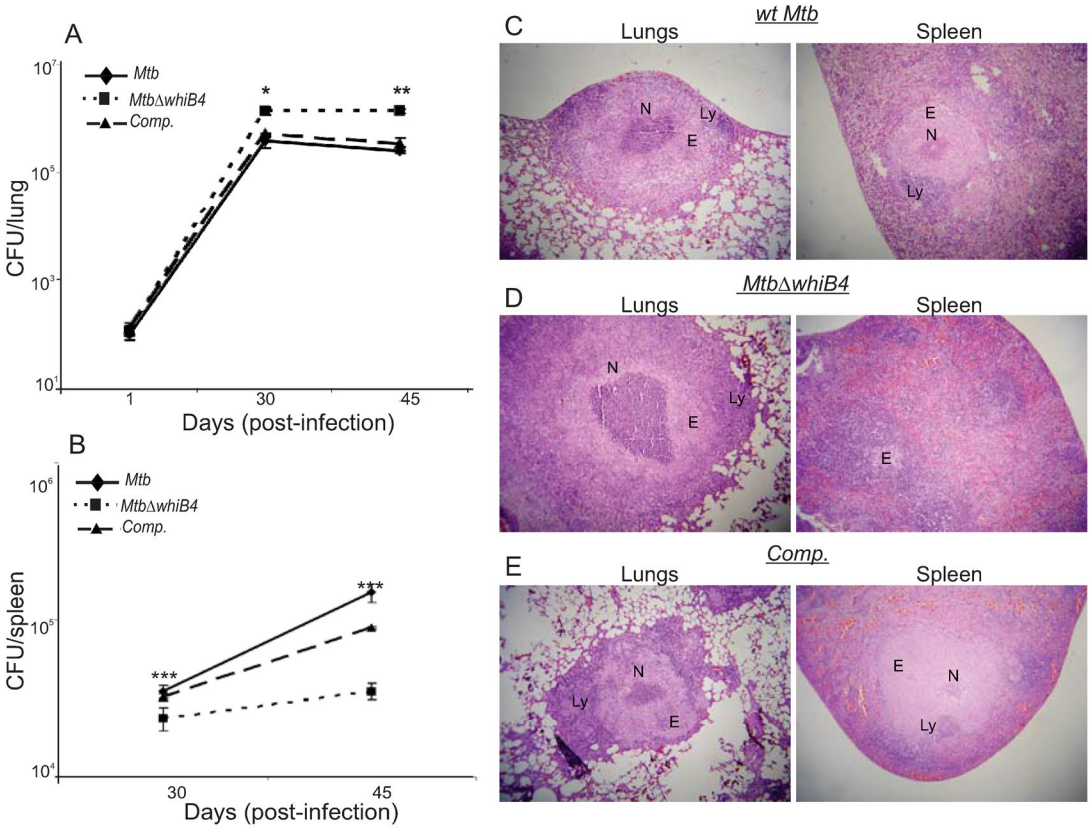

Fig. 8. WhiB4 modulates *in vivo* survival and pathology of *Mtb* in guinea pigs

Outbred Hartley guinea pigs (n=5) given an aerosol challenge of *Mtb* were assessed for bacterial burden in lungs (A) and spleen (B), and for the severity of lung and spleen pathology (C, D and E). Statistical significance for the pulmonic and splenic bacterial load was obtained by comparing wt *Mtb* and *MtbΔwhiB4* strains: *P<0.05, **P<0.01, ***P<0.001. Hematoxylin and eosin stained lung and spleen sections (30 days post-infection) from guinea pigs infected with wt *Mtb* (C), *MtbΔwhiB4* (D) and the *whiB4* complemented (Comp.) strains (E). The pathology sections show granulomas containing areas of necrosis (N), epithelioid cells (E), and lymphocytes (L). All images were taken at 4X magnification. Error bars represent the standard error of the mean.